

Supersaturation and Crystal Nucleation in Confined Geometries

Torsten Grünewald,[†] Lars Dähne,[‡] and Christiane A. Helm^{*,†,§}

Institut für Physikalische Chemie, Johannes Gutenberg-Universität Mainz, Jakob-Welder Weg 11, 55099 Mainz, Germany, Institut für Physikalische Chemie, Freie Universität Berlin, Takustrasse 3, 14195 Berlin, Germany, and Fachrichtung Experimentalphysik, Universität des Saarlandes, Postfach 151150, 66041 Saarbrücken, Germany

Received: October 6, 1997; In Final Form: March 27, 1998

Surface aggregation as a necessary condition for interfacially induced crystal nucleation is studied with a surface forces apparatus (SFA).^{1–3} As a model system, we use the chloride salt of the rod-shaped dye bis-(dimethylamino)hepatmethine (BDH⁺Cl[−]) in water.⁴ Even when the bulk solution is 3 orders of magnitude below saturation concentration, in a molecularly thin gap we find a structural oscillatory interaction force, whose periodicity and viscosity indicate a supersaturated salt solution. The increased gap concentration can be rationalized by ion-pair formation of the large molecule. If only one salt monolayer is trapped between the surfaces, optical concentration measurements yield an area coverage corresponding to freely rotating rod-shaped cations. If the surface coverage increases, the oscillatory force is replaced by a purely repulsive force indicative of ion surface aggregation. These salt aggregates thicken during an experiment. Eventually, crystallization occurs at a surface separation of about 100 nm. If the bulk concentration is only 1 order of magnitude below saturation, salt crystallization occurs at the first approach of the surfaces, indicating pronounced aggregation on the isolated surfaces.

Introduction

The morphology of growing crystals from solution has been investigated thoroughly;²³ however, little is known on a molecular basis about the necessary and sufficient conditions for crystal nucleation itself. The dissolved ions have to accumulate and then arrange in the crystalline pattern to form the nucleus. Recently, it was shown that nucleation is promoted by a structured surface which offers a template and may influence the lattice structure.^{5,24} Furthermore, for rod-shaped molecules it was shown theoretically that adjacent to the interface the concentration may be further increased due to the steric attractions.⁶

In the simplest, purely electrostatic view a comparison between the free energy of the monovalent ions—either dissolved or in the crystal—reads⁷

$$G_{\text{solv}} = - \sum_{\text{all ions}} \frac{e^2 a_i}{8\pi\epsilon_0\epsilon_r R_i} \quad \text{and} \quad G_{\text{crystal}} = -\alpha \frac{e^2}{4\pi\epsilon_0 a} \quad (1)$$

(ϵ_0 is the dielectric constant of vacuum and ϵ_r that of water. R_i is the radius of the ion i and a_i its activity coefficient; a_i approaches unity in very dilute solutions. α is the Madelung constant of the crystalline lattice and a its smallest distance.)

The energy of ions in aqueous solutions is decreased by about 2 orders of magnitude compared to the vacuum, due to the high dielectric constant of water ($\epsilon_r = 78.5$). At saturation concentration, crystal and solution are at equilibrium, $G_{\text{crystal}} = G_{\text{solv}}$. A supersaturated solution is energetically unstable, $G_{\text{crystal}} < G_{\text{solv}}$, meaning that equally charged ions are no longer strongly

repelled. The attraction between co-ions is mediated by counterions. Therefore, ions aggregate and a crystal nucleates. However, in systems kinetically trapped (with a very high nucleation energy) an amorphous glass is formed. Note that the solvation energy of ions close to an interface is different from the bulk phase, mainly due to the much lower dielectric constant of the solid (mica: $\epsilon_r = 2.5$).

Materials and Methods

For various reasons, BDHCl is a suitable model system for a solidification study. The solubility (0.0742 mol/L) is conveniently low.⁴ The charge distribution in the rod-shaped dye is perfectly symmetric;⁸ therefore it is possible to describe the cation as a rod. Furthermore, the cationic dye is electrostatically attracted by the negatively charged mica surface. Spectroscopically, solution and crystal can be easily distinguished, since the absorption maxima differ by 130 nm.⁹ The lattice of the optically anisotropic crystal is planar,¹⁰ and the crystals tend to nucleate and grow epitaxially on mica (cf. Figure 1).

With the surface forces apparatus (SFA) the interaction force between two molecularly flat mica surfaces in a sphere on a flat geometry is measured by recording the deflection of a spring. The force normalized to the sphere radius is directly proportional to the interaction energy between two flats.¹¹

For a further characterization of the molecular thin cationic layer sandwiched between the mica surfaces, the pointwise absorption spectrum is determined. This is done by exploiting the fact that the mica sheets of equal thickness silvered on the back form a symmetrical cavity. Thus, the light field corresponding to the resonance peaks of *even* order exhibits a maximum at the position of the dye (cf. Figure 2).^{3,12} Due to absorption, the transition intensity decreases as a function of the imaginary part of the dielectric constant, $\epsilon'' = 2n\kappa$. Conveniently, the wavelength shift relative to mica/mica contact

* To whom correspondence should be addressed.

[†] Johannes Gutenberg-Universität Mainz.

[‡] Freie Universität Berlin.

[§] Universität des Saarlandes.

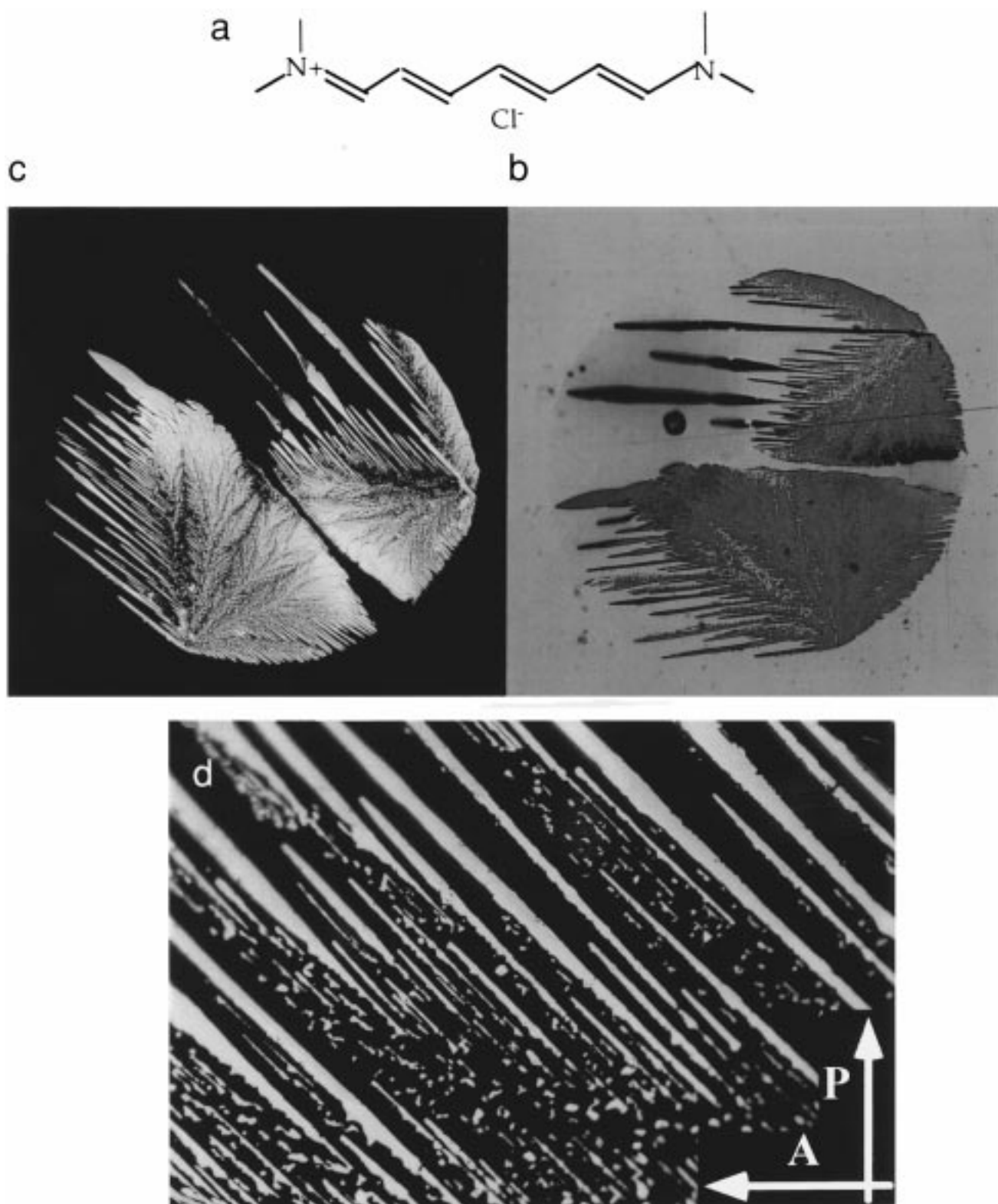


Figure 1. (a) Molecular formula of BDH^+Cl^- . (b) A BDHCl crystal grown on molecularly flat mica by condensation of a droplet of a 10^{-2} M aqueous solution as observed with a standard light microscope. The real-life colors of the solution (red) and the crystal (blue) are indicative of the shift in the absorption maximum. The crystal is viewed between crossed polarizers (Analyzer and Polarizer directions marked). (c) The droplet rotated by 45° and viewed between the same unchanged crossed polarizers. The optical anisotropy of the crystal is obvious, as well as the alignment of the mica lattice. (d) The magnification of (c) showing the epitaxial growth of the BDHCl crystals.

is determined by the real part of the dielectric constant, $\epsilon' = n^2 - \kappa^2$. Since the light field of the *odd* fringes is zero in the cavity center, their transmission is independent of the medium dielectric constant and the dye thickness can be readily determined.

Results and Discussion

First we shall concentrate on the interaction in a molecular thin gap, when the bulk concentration is still 3 orders of magnitude below the saturation concentration. For small

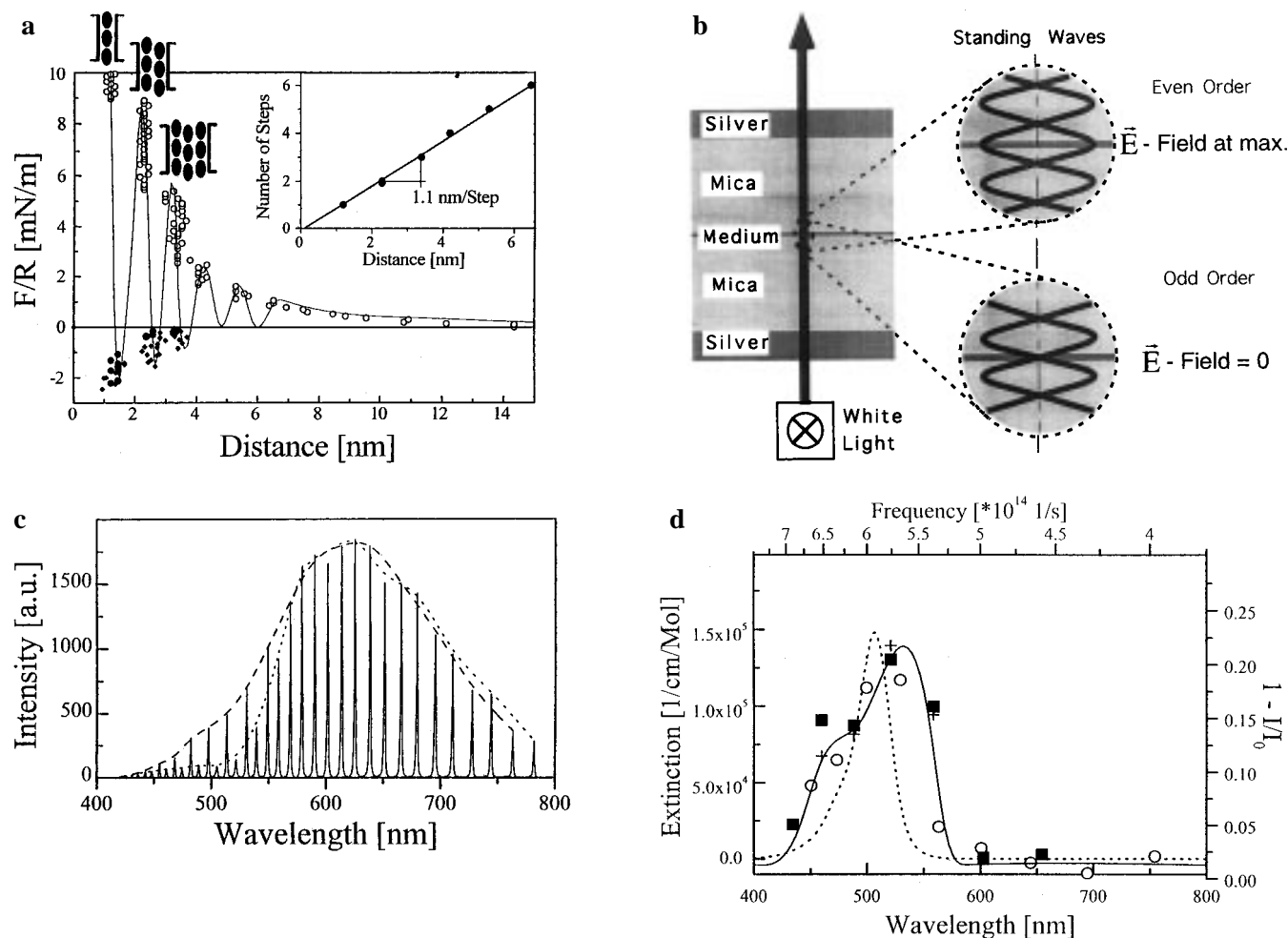


Figure 2. (a) The normalized interaction force between mica surfaces immersed in a 7×10^{-5} M BDHCl solution measured with a constant speed of 0.25 nm/s (faster compressions as applied in Figure 2 blur the oscillations). As the inset demonstrates, the periodicity is 1.1 nm, which corresponds to the diameter of a hydrated BDH⁺ molecule. (b) Principle of measuring the pointwise absorption spectrum in the SFA by decreasing the transmission intensity of the even fringes, whose light field is at a maximum in the gap. (c) Typical transmission spectrum of the cavity with about five amorphous solidified BDHCl layers between the surfaces. (d) Normalized intensity decrease of the even fringes as observed with one monolayer dye between the surfaces. Each symbol corresponds to a different experiment. The solid line is the deduced monolayer spectrum, which is described by two Gaussian profiles. Also shown is the extinction spectrum of the solution (dashed line).

monovalent ions it is known that the interaction can be very well described with the DLVO theory.¹³ For the larger rod-shaped ions, one finds a small van der Waals attraction, also. However, most prominent at close separations is a steric oscillating interaction (cf. Figure 2). On compression, separate molecular layers are removed, which can be clearly distinguished if the surfaces are approached very slowly. The periodicity of the structural force is 1.1 nm. If many approach/separation cycles are performed, the oscillatory force disappears, while the adsorbed layer thickens and a repulsive force grows.

This is a very unusual oscillatory force. Until now, all structural forces observed could be explained with the molecular dimensions of the solvent. However the periodicity we find is about a factor 4 too large,^{13,14} and we have to attribute it to the solute. The molecular dimensions of the rod-shaped dye are $1.5 \times 0.45 \times 0.35$ nm³. There seems to be no direct correlation with the periodicity, yet when taking into account the layered structure of the BDHCl tetrahydrate crystal, one finds that the thickness of a water/dye/water unit is 1.08 nm. It seems that the hydrated rod-shaped cations are oriented parallel to the interface. In the case of adsorption perpendicular to the surfaces, no absorption would be possible.

Therefore, the pointwise absorption spectrum was determined with a finite number of salt layers between the surfaces. From

Figure 3 it is obvious that the absorption spectrum of the monolayer while broadened is principally the same as that of the solution. No absorption occurs at 635 nm, the absorption maximum of the crystal.⁹ Within our resolution, we find no preferential polarization. The consistency of the values of ϵ' and ϵ'' is verified with a Kramers–Kronig analysis.¹⁵

The dye concentration in the monolayer can be deduced from the integrated absorption \mathcal{A} , according to³

$$\mathcal{A} = \frac{4\pi}{c[\text{dye}] \log_e 10} \int \nu \kappa d\nu \quad \text{and} \quad f_{\text{layer}} = \frac{6cm_e\epsilon_0}{N_A e^2} \mathcal{A} \log_e 10 \quad (2)$$

(with c the speed of light, ν the light frequency, [dye] the dye concentration, and m_e the electron mass). In this calculation, the oscillator strength of the dye is taken to be constant and independent of its surroundings (with $f_{\text{layer}} = 1.5f_{\text{solution}}$, due to the two-dimensional confinement). This approach is valid because of the completeness and orthogonality of the quantum mechanical solutions.

If only one dye monolayer is left between the surfaces, its concentration is increased by 4 orders of magnitude relative to the solution (0.7 mol/L, corresponding to 1 rod-shaped molecule per 2.2 nm²). This concentration increase is quite amazing and

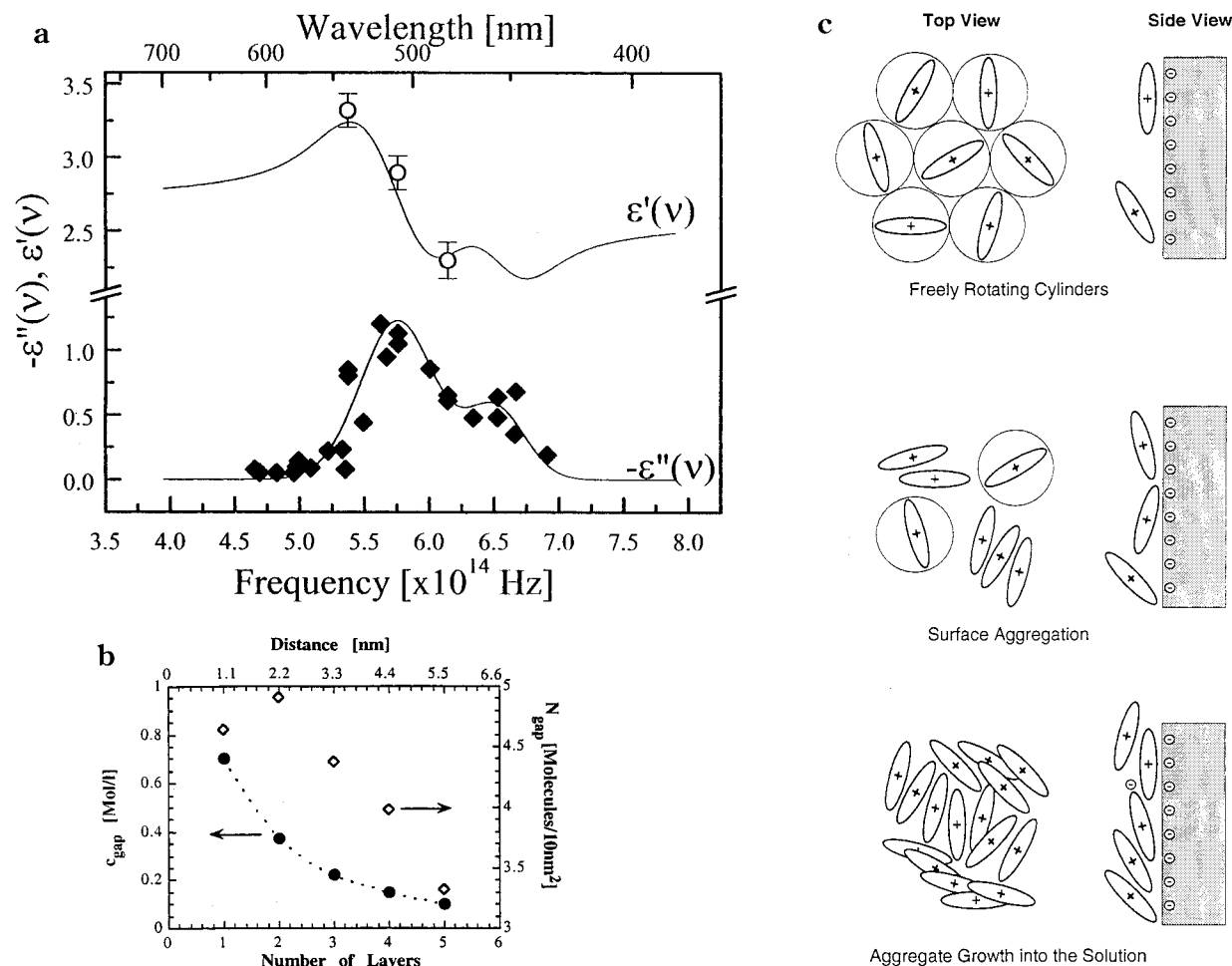


Figure 3. (a) Real and imaginary part of the dielectric constant of a monolayer based on the measurements shown in Figure 2d. The experimental points obtained for the real part of the dielectric constant correspond to the circles of Figure 2d. In this experiment it was possible to measure not only the intensity decrease of the even fringe but also the absolute wavelength shifts of the even fringes relative to mica/mica contact. (b) Total integrated amount of BDH⁺ molecules between the surfaces, N_{gap} (diamonds), as deduced from the integrated absorption as a function of gap width, i.e., number of layers. Also shown is the average concentration, c_{gap} (circles), between the surfaces. The dotted line is a guide for the eyes. (c) Schematic of the arrangement of the rod-shaped cations on a mica surface on increasing concentration. Top: When the molecules still freely rotate, the mica surfaces can approach until only one molecular layer is left and van der Waals attraction is observed. Center: On increase of the interfacial concentration, surface aggregates form, and the interaction between the surfaces is governed by a short-range repulsion. Bottom: The aggregates grow toward the solutions; simultaneously the repulsion increases in range. If two surfaces approach, crystallization occurs.

2 orders of magnitude larger than the one expected for electrostatical reasons neglecting ion binding (at most $e^{\psi/kT} \leq 150$). If we describe the molecules as freely rotating sticks,¹⁶ we would expect an area per molecule of 1.9 nm². Thus, the dye molecules in the gap appear to be isolated and not to interact laterally.

On step-by-step increase of the surface separation D , the total number of cations per unit area between the surfaces, N_{gap} , decreases. This is not expected from the DLVO theory. DLVO theory is based on the electroneutrality condition. Thus, the dye concentration in the gap between the surfaces should approach the bulk concentration at large distances according to $c_{\text{gap}} = c_{\text{bulk}} + \sigma_{\text{surplus}}/D$. If we assume a constant negative surface charge σ for mica,¹¹ the total cation concentration in the gap is increased relative to the bulk concentration by $\sigma_{\text{surplus}}/D$ (in terms of equations, the electroneutrality condition reads $\sigma_{\text{surplus}} + \sigma = 0$). The assumption of a constant surface charge σ of mica leads to a strong increase in the surface potential on approach of the charged surfaces. The other extreme case to be considered is the one of constant surface potential. Here the surface charge σ decreases on approach. In this case, σ_{surplus} is no longer constant, but decreases at very

close separations due to ion binding. Thus c_{gap} may exhibit a small maximum before leveling off at c_{bulk} .

We measure $N_{\text{gap}} = Dc_{\text{gap}}$, the total number of cations per unit area between the surfaces. Therefore, N_{gap} should almost monotonically increase as $N_{\text{gap}} = Dc_{\text{bulk}} + \sigma_{\text{surplus}}$. We find the opposite effect, with the exception of the first layer; N_{gap} decreases on surface separation (cf. Figure 3). There is obviously a strong attraction of the cations toward a surface; this attraction is amplified in the gap.

This behavior cannot be explained only by a large binding constant (i.e. the ion-exchange model) between dye cations and surface, because the accompanied changes in the surface potential do not lead to a structural force with a range of about five molecular diameters. Theoretical calculations¹⁷ show that the double-layer force can exhibit an additional minimum when the counterions are large enough. This was shown in the "primitive model",¹⁷ where all counterions are desorbed from the surface and no additional salt is added. A necessary condition for the occurrence of the minimum was a substantially decreased dielectric constant. This assumption may be reasonable, since the dielectric constant of concentrated salt solutions

is lowered by a factor 2 or more. Probably, in our experiments, the dielectric constant is not homogeneous between the walls.

We can only speculate about the amount of Cl^- coions between the surfaces. However, it may be very crucial to realize that the gap concentration c_{gap} exceeds the saturation concentration by a factor 10 for the monolayer and still by a factor 1.3 if the gap consists of five layers. If we assume that the Cl^- concentration is of the same order of magnitude as the BDH^+ concentration, the solution in the gap is supersaturated. There should be a pronounced ion-ion interaction which causes an additional attraction between the co-ions. The shift of the absorption maximum to longer wavelengths as observed in Figure 2 is indicative of pronounced surface interactions,¹⁸ yet it does not yield very specific information. Concluding, we think that between the mica surfaces the Gibbs energy of solvation G_{solv} is decreased compared to the bulk solution, even though the detailed physical reasons are not obvious.

When the surfaces are separated, the ion-pairs and/or the BDH^+ molecules from the supersaturated gap solution may either dissolve again in the bulk or solidify on the surface. With very dilute bulk solutions, we find in the beginning of an experiment a van der Waals attraction and a BDH^+ concentration in agreement with the model of freely rotating rods. Initially, surface aggregates can be excluded. But the eventual disappearance of the van der Waals attractions, the optically observed increase of trapped cationic dye molecules, and the growth of a repulsive force indicate the formation of surface aggregates. Furthermore, the drift into contact found in every single experiment suggests that molecules from the solution deposit continuously on the surface. If this is so, we have to assume that the immobilized surface aggregates offer additional adsorption sites, leading to the formation and the subsequent continuous growth of an adsorbed layer during many approach/separation cycles. This idea is supported by the fact that the adsorbed layer thickens when the surfaces are slid laterally against each other.¹⁹

With an increase of the cation concentration in the bulk the van der Waals attraction disappears, a feature well-known from small monovalent ions,^{20,21} which is attributed to strong binding of hydrated cations. The observed repulsive force (i.e., hydration force) is believed to be due to the energy needed to dehydrate the bound cations, which presumably retain some of their hydration water on binding. We find that the "hydration force" is observed as soon as the gap concentration is too high to allow the rods to rotate freely. Thus we have to conclude that (probably nanosized) surface aggregates form.

To characterize the isolated surfaces, one can try to determine the surface potential from the size of the long-range electrostatic interaction force F_0 . For small monovalent ions this ansatz was very successful. Thus, the surface potentials could be explained in the framework of an ion-exchange model, based on simple mass-action laws.^{11,21}

The long-range interaction force between two negatively charged mica surfaces in BDHCl solution appears to be typical for DLVO-type behavior (cf. Figure 4):

$$F/R = -\frac{A}{D^2} + F_0 \text{Re}^{-\kappa D} \quad (3)$$

It is a superposition of van der Waals attraction and electrostatic repulsion; the former is proportional to the Hamaker constant A and inversely proportional to the square of the surface separation D . The latter decays exponentially with the Debye length $1/\kappa$, which is a function of the bulk concentration c_{bulk} and is independent of surface properties. The Debye length

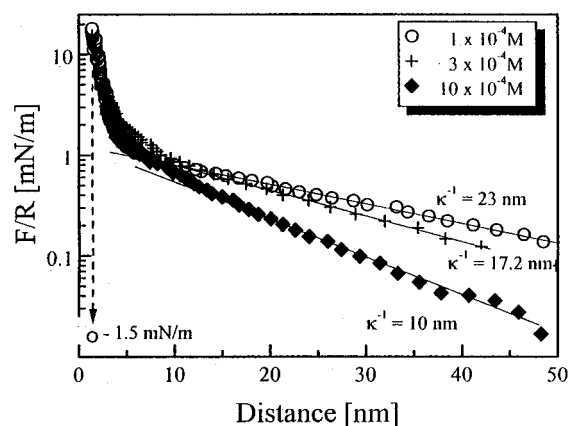


Figure 4. The normalized interaction force between mica surfaces for the BDHCl concentrations indicated. Typically for an electrostatic repulsion, the force increases exponentially. The theoretically expected Debye lengths (30.1, 17.3, and 9.5 nm for 10^{-4} , 3×10^{-4} , and 10^{-3} mol/L, respectively) are found.

decreases as expected on concentration increase. Obviously, the rod-shaped BDH^+ can be treated at large surface separations as a point charge. Yet the deduced surface potentials are much smaller than those found with small monovalent ions in the solution, indicating a binding constant about an order of magnitude larger. However, in the concentration range shown in Figure 4, in the ion-exchange model the deduced area per dye molecule decreases from 1.1 nm^2 to 0.5 nm^2 . These numbers disagree with a sterically flat adsorption layer. Obviously, the bound layer extends into the solution and shields the surface potential very efficiently. Thus, for the long-range part of the interaction law we find contradictions if we try to describe the surface potential quantitatively on the basis of DLVO theory.

The cleavage work of mica is mainly due to the electrostatic force that holds the layers together. During cleavage potassium ions have to choose sides and end up in a situation (neglecting polarization effects) where the mica charges are somewhat delocalized and the potassium ions are not locally neutralized. The BDH^+ ion, on the other hand, has a very high internal polarizability and can better adjust to the local charge distribution. This could cause a substantial extra contribution to the adsorption energy, explaining the low surface potential and possibly also the increased BDH^+ concentration in the gap.

After various approach/separation cycles, the surfaces cannot be approached as closely as before due to the appearance of a strong additional repulsive force. If one assumes the plane of charge origin to be constant, the surface potential increases. Yet it is more likely that more BDH^+ immobilizes on the surface, and the plane of charge origin is moved further away from the mica surfaces, since the optically determined amount of cations between the surfaces increases simultaneously. Thus, one has to conclude that the adsorbed layer thickens. The surface aggregates grow into the solution. Finally, crystallization occurs.

With increasing bulk concentration, both the surface aggregation and the subsequent crystallization accelerate. Two orders of magnitude below the saturation concentration only very few force runs can be performed. Yet, presumably for kinetic reasons, crystallization never occurs in a molecular thin gap. Actually, two different crystal nucleation geometries can be distinguished: in the center for slightly separated surfaces ($D \approx 100 \text{ nm}$) or at the edge of the contact zone (also at $D \approx 100 \text{ nm}$). In the latter case the nucleus grows quickly toward the center. Note that in the supersaturated salt solution a BDHCl ion-pair is solubilized by about 100 water molecules, which are

freed on crystal nucleation and cause large local flows. Thus, the growing crystals separate the surfaces with a large repulsive force.

Obviously, nucleation would be facilitated by epitactic growth (cf. Figure 1). In the experiments presented so far (cf. Figures 2–4), the lattice planes are oriented randomly against each other, as was verified by checking the mica birefringence.²² Experiments with aligned mica crystals lead usually to immediate crystallization at a surface separation of ≈ 100 nm.

Conclusions and Implications

Concluding, we find an indirect correlation between the bulk concentration of the rod-shaped cation and the concentration at an *isolated* surface. Initially, the cation adsorption does grow on increase of the bulk concentration. However, if the coverage is so large that the rod-shaped cations start to interact, (presumably nanosized) surface aggregates form. Then the van der Waals attraction is replaced by a short-range repulsion. The formation of immobile surface aggregates is hastened by the approach/separation cycles in the SFA. The cations accumulate in a molecularly thin gap. If the surfaces are separated again, some cations join the surface aggregates promoting their growth. Eventually a crystal nucleates.

The mechanism outlined above appears to apply to many large ions with low solubility. Experimentally, surface aggregates are observed for a wide range of ions. CaCl_2 in kitchen appliances is a prominent example; water soluble dyes seem to stick at every surface. Theoretically, a high surface binding constant is essential to induce a supersaturated solution in a molecularly thin layer.

Acknowledgment. First of all we wish to thank Alan Berman and Jacob Israelachvili for their hospitality and their support with the sliding experiments. We thank Helmuth Möhwald for many fruitful discussions. The financial support of the Sonderforschungsbereich 262 and the Ministerium für

Bildung und Forschung (F+E-Vorhaben 13N6284) are gratefully acknowledged.

References and Notes

- (1) Israelachvili, J. N.; Tabor, D. *Proc. R. Soc. London A* **1972**, *331*, 19–38.
- (2) Grünwald, T.; Helm, C. A. *Langmuir* **1996**, *12*, 3885–3890.
- (3) Müller, C.; Mächtle, P.; Helm, C. A. *J. Phys. Chem.* **1994**, *94*, 11119–11125.
- (4) Dähne, L.; Reck, G. *Angew. Chem.* **1995**, *107*, 735–737.
- (5) Blaaderen, A. v.; Wiltzius, P. *Science* **1995**, *270*, 1177–1179.
- (6) Yaman, K.; Pincus, P.; Marques, C. M. *Phys. Rev. Lett.* **1997**, *78*, 4514–4517.
- (7) Atkins, P. W. *Physical Chemistry*; W. H. Freeman and Company: New York, 1990.
- (8) Försterling, H.-D.; Kuhn, H. *Moleküle und Molekülanhäufungen*; Springer-Verlag: Berlin, 1983.
- (9) Dähne, L.; Horvath, A.; Weiser, G.; Reck, G. *Adv. Mater.* **1996**, *8*, 486–490.
- (10) Groth, P. *Acta Chem. Scand.* **1987**, *B41*, 547–550.
- (11) Israelachvili, J. N. *Intermolecular and Surface Forces*; Academic Press: London, 1991.
- (12) Mächtle, P.; Müller, C.; Helm, C. A. *J. Phys. II Fr.* **1994**, *4*, 481–500.
- (13) Evans, F.; Wennerström, H. *The Colloidal Domain: Where Physics, Biology, and Technology Meet*; VCH: Weinheim, New York, 1994.
- (14) Israelachvili, J.; Pashley, R. *Nature* **1983**, *306*, 249–250.
- (15) Yeh, P. *Optical Waves in Layered Media*; John Wiley: New York, 1988.
- (16) Lekkerkerker, H. N. W.; Buining, B.; Buitenhuis, J.; Vroege, G. J.; Stroobants, A. Liquid crystal phase transitions in dispersions of rodlike colloidal particles. In *Observation, Prediction and Simulation of Phase Transitions in Complex Fluids*; Baus, M., et al., Eds.; Kluwer Academic Publishers: Netherlands, 1995; pp 53–112.
- (17) Delville, A.; Pellenq, R. J. M. *J. Phys. Chem. B* **1997**, *101*, 8584–5894.
- (18) Dähne, L. *J. Am. Chem. Soc.* **1995**, *117*, 12855–12860.
- (19) Israelachvili, J. N.; Chen, Y.-L.; Yoshizawa, H. *J. Adhesion Sci. Technol.* **1994**, *8*, 1231.
- (20) Pashley, R. M. *J. Colloid Interface Sci.* **1981**, *80*, 153–162.
- (21) Pashley, R. M. *J. Colloid Interface Sci.* **1981**, *83*, 531–546.
- (22) McGuigan, P.; Israelachvili, J. N. *J. Mater. Res.* **1990**, *5*, 2232–2243.
- (23) Kurz, W.; Fisher, D. J. *Fundamentals of Solidification*; Trans Tech Publications Ltd: Switzerland, 1989.
- (24) Jacquemain, D.; Wolf, S. G.; Leveiller, F.; Deutsch, M.; Kjaer, K.; Als-Nielsen, J.; Lahav, M.; Leiserowitz, L. *Angew. Chem., Int. Ed. Engl.* **1992**, *31*, 130–152.